PAPER

Scalability of dark current in silicon PIN photodiode

To cite this article: Ya-Jie Feng *et al* 2018 *Chinese Phys. B* **27** 048501

Scalability of dark current in silicon PIN photodiode*

Ya-Jie Feng(丰亚洁)[1,2], Chong Li(李冲)[2], Qiao-Li Liu(刘巧莉)[2], Hua-Qiang Wang(王华强)[2], An-Qi Hu(胡安琪)[1], Xiao-Ying He(何晓颖)[2,†], and Xia Guo(郭霞)[1,‡]

[1] *School of Electronic Engineering, State Key Laboratory of Information Photonics and Optical Communications, Beijing University of Posts and Telecommunications, Beijing Key Laboratory of Work Safety Intelligent Monitoring, Beijing* 100876, *China*

[2] *Department of Information, Beijing University of Technology, Beijing* 100124, *China*

(Received 31 July 2017; revised manuscript received 11 January 2018; published online 10 March 2018)

The mechanism for electrical conduction is investigated by the dark temperature-dependent current–voltage characteristics of Si PIN photodiodes with different photosensitive areas. The characteristic tunneling energy E_{00} can be obtained to be 1.40 meV, 1.53 meV, 1.74 meV, 1.87 meV, and 2.01 meV, respectively, for the photodiodes with $L = 0.25$ mm, 0.5 mm, 1 mm, 1.5 mm, and 2 mm by fitting the ideality factor n versus temperature curves according to the tunneling-enhanced recombination mechanism. The trap-assisted tunneling-enhanced recombination in the i-layer plays an important role in our device, which is consistent with the experimental result that area-dependent leakage current is dominant with the side length larger than 1 mm of the photosensitive area. Our results reveal that the quality of the bulk material plays an important role in the electrical conduction mechanism of the devices with the side length larger than 1 mm of the photosensitive area.

Keywords: silicon PIN photodiodes, dark current, tunneling enhanced

PACS: 85.30.–z, 85.60.Dw, 85.60.Gz **DOI:** 10.1088/1674-1056/27/4/048501

1. Introduction

Silicon PIN photodiodes have wide applications in IR remote controls, industrial electronics, defense, security, medical and scientific instruments, etc. due to their high sensitivity and low cost.[1–3] The sensitivity of a photodetector determines the lowest light intensity that can be detected, which reflects the image definition.[4] The leakage current directly relates to the sensitivity of the detector, hence, it is important to understand the electrical conduction mechanism inside. It is generally believed that the leakage current is composed of bulk diffusion current, generation–recombination current of minority carriers in the space-charge region,[5,6] tunneling current at the p/i interface, etc.[7] Besides the material quality and electric-field design inside, the perimeter-to-area of the photosensitive region also influences the leakage current of the device.[8–10] In this paper, the quantitative analyses of the electrical properties of the Si PIN photodiodes with different photosensitive areas are demonstrated by the temperature-dependent current–voltage (I–V) measurement method. It is shown that the trap-assisted recombination plays a more important role in the dark carrier transport mechanism with the increase of the device size. The scalability study indicates that the perimeter of the photosensitive region affects the dark current more than their photosensitive area when the side length of the photosensitive region is below 0.5 mm.

2. Experiments

The cross-sectional diagram of the Si PIN photodetector studied in this paper is illustrated in Fig. 1. The guard ring with phosphor ion implantation was used in order to avoid the dark current generated from the wafer-dicing damage. The SiN_x was grown by low pressure chemical vapor deposition (LPCVD) as an antireflection coating layer with a transmittance of 95.5% on the photosensitive surface. The surface regions without implantation were covered by passivating oxide layers. The side lengths (L) of the square photosensitive region were designed to be 0.25 mm, 0.5 mm, 1 mm, 1.5 mm, and 2 mm, respectively. The temperature-dependent I–V curves were measured by using the apparatus consisting of a closed-cycle helium cryostat from the JANIS company, a programmable temperature controller and a Keithley 4200, a source-measure meter in the dark environment.

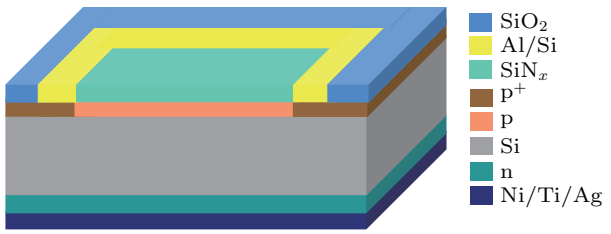

Fig. 1. (color online) Cross-sectional diagram of Si PIN photodiode. Photosensitive area is covered by SiN antireflection coating layer with transmittance of 95.5%.

*Project supported by the National Key Research and Development Program of China (Grant No. 2017YFF0104801) and the National Natural Science Foundation of China (Grant Nos. 61335004, 61675046, and 61505003).

†Corresponding author. E-mail: xyhe@bjut.edu.cn

‡Corresponding author. E-mail: guox@bupt.edu.cn

3. Results and discussion

Figure 2(a) shows the forward dark I–V curves for the photodiodes with $L = 0.25$ mm, 0.5 mm, 1 mm, 1.5 mm, and 2 mm under the room temperature. The ideality factors are calculated to be 1.055, 1.062, 1.054, 1.047, and 1.056, respectively, according to the following expression[11,12]

$$n = \frac{q}{kT}\frac{\partial V}{\partial \ln I}.$$

All the ideality factor values of these PIN photodetectors are close to 1, which indicates the diffusion current dominants the carrier transport under the room temperature. Figure 2(b) shows the dark reverse I–V curves under the room temperature for all the five devices. Generally, for Si photodiodes used in the security inspection, the reverse bias is 0 V due to the high responsitivity, which reaches to 0.65 A/W for the photodiodes used in this paper. The reverse curves each can be devided into three parts as shown in Fig. 2(b). For parts I and III, the experimental data are in good agreement with the mathematical model that describes the diffusion current from the quasi-neutral area and the generation current from the depletion area for the whole curve.[13] For part II, there is a crook on each curve, which is attributed to the contamination in the Ohmic contact interface, revealed by the frequency-dependent capacitance-voltage measurement.[14]

The reverse dark current can be decomposed into the length-dependent part generated from the edge of p–n junction, the area-dependent part generated in or close to the depletion region, and a compensation current which depends on neither area nor circumference.[15] Thus, the total leakage current with the side length can be expressed as follows:

$$I_{\mathrm{R}} = J_{\mathrm{peri}} 4L + J_{\mathrm{area}} \cdot L^2 + I_{\mathrm{offset}}, \tag{1}$$

where I_{R} is the total reverse leakage current of the photodiodes; J_{peri} is the current density per mm generated at the surface, J_{area} is the current density generated in the area; I_{offset} is the current offset. Figure 2(c) shows the reverse currents versus side length at −1 V, −10 V, −20 V, and −30 V on the side length L of the photodiodes. The data are extracted from Fig. 2(b) and denoted by dots. The solid curves are the fitting curves with these dots according to Eq. (1), which agree well with the experimental data. The ratio of the length-dependent ($I_{\mathrm{peri}}/I_{\mathrm{R}}$) and area-dependent leakage current ($I_{\mathrm{area}}/I_{\mathrm{R}}$) can be extracted from the fitting. For the devices with $L = 0.25$ mm and 0.5 mm at the voltage lower than −10 V, the main leakage comes from the perimeter for the small device at lower bias. While for the devices with $L = 1$ mm, 1.5 mm, and 2 mm, the leakage from the bulk material is the main leakage source. For the device with $L = 2$ mm at −1 V, the area-dependent leakage current can reach to 81% and increases slowly with bias increasing.

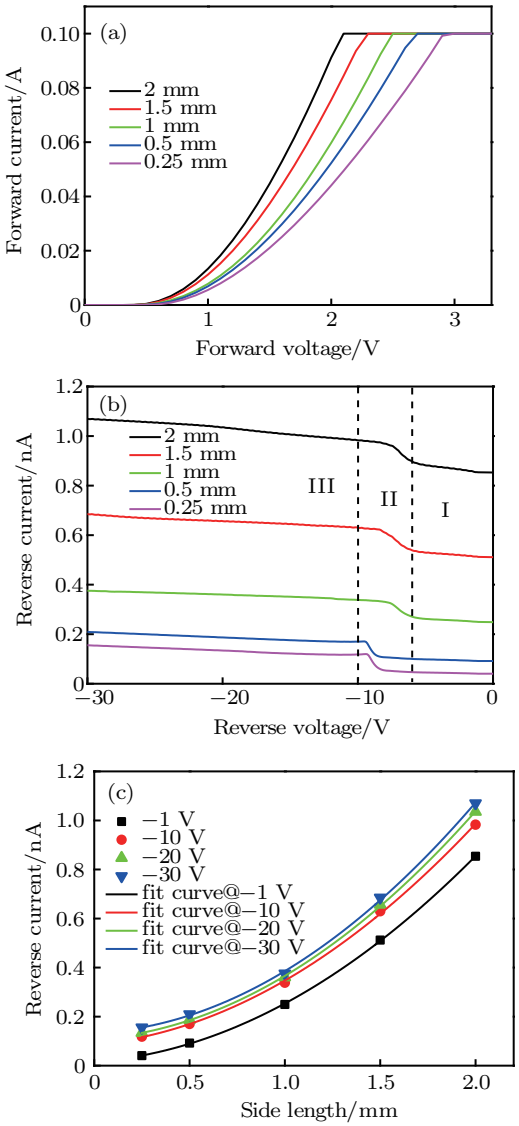

Fig. 2. (color online) Dark I–V curves measured under the room temperature for Si photodiodes with $L = 0.25$ mm, 0.5 mm, 1 mm, 1.5 mm, and 2 mm, respectively. (a) Forward biased. (b) Reverse biased. (c) Dependence of reverse current on the side length of the photosensitive area with reverse bias voltages of −1 V, −10 V, −20 V, and −30 V. The lines are the fitting curves according to Eq. (1).

In order to further study the electric conduction behaviors in the Si photodiodes, the temperature-dependent I–V curves are measured. Figure 3(a) presents the dark forward I–V measurement results from 40 K to 300 K by taking the device with $L = 2$ mm for example. The slopes of the $\log I$–V plots are calculated to be 58.06, 59.52, 57.37, 47.02, 43.74, 43.18, 42.11, 39.61, and 37.68, respectively, which are sensitive to temperature. The values of corresponding ideality factor n are 6.18, 2.67, 1.93, 1.65, 1.33, 1.12, 1.07, 1.05, and 1.02, respectively, which decrease with temperature increasing. The recombination process may occur in the space charge region or at the p–i interface. It can be noted that the slope values of $\log I$–V curves at 40 K, 80 K, and 120 K are very close to each other, which indicates that the recombination process is enhanced by tunneling assisted by defects at or close to the junc-

tion interface.[16]

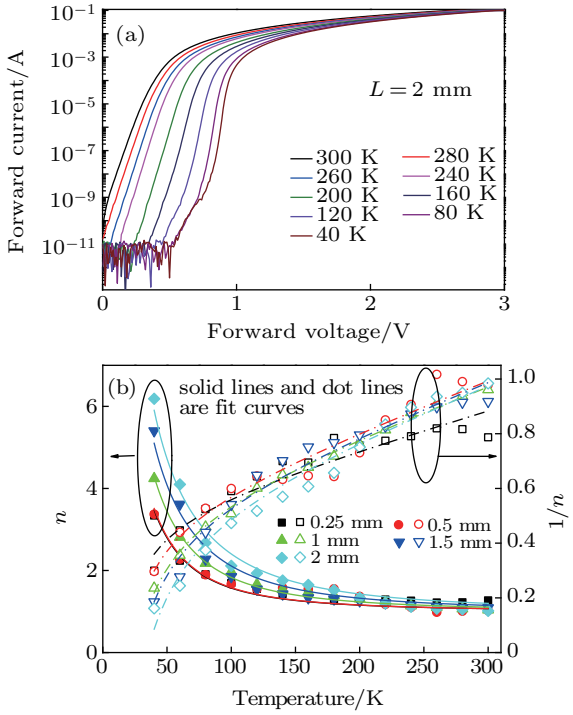

Fig. 3. (color online) (a) Temperature-dependent forward I–V curves in semi-logarithmic coordinates for photodiode with $L = 2$ mm from 40 K to 300 K. (b) Variations of ideality factor n with temperature (dots); solid lines represent fitting results according to Eq. (2). Empty circles denote reciprocals of ideality factor; dotted lines refer to fitting results according to Eq. (3).

The tunneling-enhanced recombination assisted by defects or traps in the bulk material or close to the junction interface can be expressed, respectively, as[17–21]

$$n = \frac{E_{00}}{kT} \coth\left(\frac{E_{00}}{kT}\right), \tag{2}$$

$$\frac{1}{n} = \frac{1}{2}\left(1 - \frac{E_{00}^2}{3(kT)^2} + \frac{T}{T^*}\right), \tag{3}$$

where E_{00} is the characteristic tunneling energy, and T is the characteristic temperature. When the E_{00} is close to 0 in Eq. (3), the recombination process is of the classical Shockley–Read–Hall recombination.

Figure 3(b) shows the relationships of n versus T and $1/n$ versus T, and their corresponding fitting results which are denoted by lines. It is found that the experimental data fit very well for the n and T relationship to the theoretical expression of Eq. (2), which describes the tunneling-enhanced interface recombination mechanism for all the devices. For the fitting according to Eq. (3), the experimental data also fit well for all the devices. According to the fitting results of Eq. (3) , the values of E_{00} are 1.40 meV, 1.53 meV, 1.74 meV, 1.87 meV, and 2.01 meV, respectively, for the photodiodes with $L = 0.25$ mm, 0.5 mm, 1 mm, 1.5 mm, and 2 mm. The characteristic tunneling energy increases with L increasing, which indicates that the tunneling process becomes easier with length increasing, which is consistent with the conclusion that area-dependent leakage current is dominant with the side length larger than 1 mm of the photosensitive area.

4. Conclusions

In this paper, the scalibity of the electrical conduction mechanism has been investigated for the Si PIN photodiode. The forward temperature-dependent I–V measurement results demonstrate that trap-assistant recombination can be used to explain the electronic loss mechanism. The quality of the bulk material plays an important role in the electrical conduction mechanism for the devices with the side length larger than 1 mm of the photosensitive area.

References

[1] Jiang J, Xu Z, Lin J and Liu G L 2016 *J. Sensors* **2016** 1
[2] Guo X, Liu Q, Zhou H, Luan X, Li C, Hu Z, Hu A and He X 2017 *IEEE Electron Dev. Lett.* **39** 228
[3] Nazififard M, Suh K Y and Mahmoudieh A 2016 *Rev. Sci. Instrum.* **87** 073502
[4] Bao C, Chen Z, Fang Y, Wei H, Deng Y, Xiao X, Li L and Huang J 2017 *Adv. Mater.* **29** 1703209
[5] Sze S M and Ng K K 2006 *Physics of Semiconductor Devices* 3rd edn. (John Wiley & Sons: John Wiley & Sons) p. 97
[6] Arch J and Fonash S 1992 *Appl. Phys. Lett.* **60** 757
[7] Hegedus S S, Salzman N and Fagen E 1988 *J. Appl. Phys.* **63** 5126
[8] Murakami Y, Satoh Y, Furuya H and Shingyouji T 1998 *J. Appl. Phys.* **84** 3175
[9] Poyai A, Simoen E, Claeys C and Czerwinski A 2000 *Mater. Sci. Eng. B* **73** 191
[10] Li T, Wang Y, Li Y F, Tang H J, Li X and Gong H M 2010 *J. Optoelectron. Laser* **21** 500
[11] Chen F P, Zhang Y M, Zhang Y M, Tang X Y, Wang Y H and Chen W H 2011 *Chin. Phys. B* **20** 117301
[12] Chen F P, Zhang Y M, Lv H L, Zhang Y M and Huang J H 2010 *Chin. Phys. B* **19** 097107
[13] Nadenau V, Rau U, Jasenek A and Schock H W 2000 *J. Appl. Phys.* **87** 584
[14] Guo X, Feng Y, Liu Q, Wang H, Li C, Hu Z and He X 2017 *IEEE J. Electron Dev. Soc.* **5** 390
[15] Loukianova N V, Folkerts H O, Maas J P, Verbugt D W, Mierop A J, Hoekstra W, Roks E and Theuwissen A J 2003 *IEEE Trans. Electron Dev.* **50** 77
[16] Dalapati P, Manik N B and Basu A N 2014 *J. Semicond.* **35** 082001
[17] Dalapati P, Manik N B and Basu A N 2015 *Cryogenic.* **65** 10
[18] Sellai A 2008 *ICSE* 2008 *IEEE International Conference*, Johor Bahru, November 2008, Malaysia, p. 267
[19] Pattabi M, Krishnan S and Sanjeev G 2007 *Sol. Energy Mater. Sol. Cells* **91** 1521
[20] Padovani F and Stratton R 1966 *Solid-State Electron.* **9** 695
[21] Zhong J, Yao Y, Zheng Y, Yang F, Ni Y Q, He Z Y, Shen Z, Zhou G L, Zhou D Q, Wu Z S, Zhang B J and Liu Y 2015 *Chin. Phys. B* **24** 097303